

Article

Tailoring Basalt Fibers and E-Glass Fibers as Reinforcements for Increased Impact Resistance

Elango Natarajan ^{1,*}, Santhosh Mozhuguan Sekar ¹, Kalaimani Markandan ¹, Chun Kit Ang ¹
and Gérald Franz ^{2,*}

¹ Faculty of Engineering, Technology and Built Environment, UCSI University, Kuala Lumpur 56000, Malaysia; mozhuguan.santhosh@gmail.com (S.M.S.); kalaimani@ucsiuniversity.edu.my (K.M.); angck@ucsiuniversity.edu.my (C.K.A.)

² Laboratoire des Technologies Innovantes, UR UPJV 3899, Avenue des Facultés, Le Bailly, 80025 Amiens, France

* Correspondence: cad.elango.n@gmail.com (E.N.); gerald.franz@u-picardie.fr (G.F.)

Abstract: The usage of basalt fiber in the engineering industries has gained significant interest due to its characteristics such as alkali resistance and enhanced mechanical properties. Similarly, E-glass-fiber-reinforced composites have been widely used in the fabrication of electrically resistive industrial components such as switches, circuit panels, and covering cases. In the present study, the tensile, flexural, thermogravimetric, and low-velocity impact characteristics of various percentages of basalt/E-glass-fiber-reinforced polymer composites fabricated via vacuum-assisted resin transfer molding were investigated. The results show that a higher volume percentage of basalt (39%) significantly enhances the impact resistance up to 45% with a moderate improvement in flexural properties. The higher the vol % of E-glass (40%), the more the tensile and flexural properties are increased, i.e., 185 N/mm² and 227.87 N/mm², respectively. It is concluded that by choosing the optimum hybridization method, impact resistance and other mechanical properties can be improved significantly. The thermogravimetric analysis results show that PC313534 (35 vol % basalt and 34 vol % E-glass) possesses the lowest decomposition temperature of 381.10 °C. The results from the present study indicate that the polymer composite fabricated in the present study is suitable for applications where higher structural-load-resistive properties are required.

Keywords: polymer composites; sustainable manufacturing; product innovation; eco-friendly; vacuum-assisted resin transfer molding



Citation: Natarajan, E.; Mozhuguan Sekar, S.; Markandan, K.; Ang, C.K.; Franz, G. Tailoring Basalt Fibers and E-Glass Fibers as Reinforcements for Increased Impact Resistance. *J.*

Compos. Sci. **2024**, *8*, 137. <https://doi.org/10.3390/jcs8040137>

Academic Editor: Francesco Tornabene

Received: 24 February 2024

Revised: 20 March 2024

Accepted: 7 April 2024

Published: 9 April 2024



Copyright: © 2024 by the authors. Licensee MDPI, Basel, Switzerland. This article is an open access article distributed under the terms and conditions of the Creative Commons Attribution (CC BY) license (<https://creativecommons.org/licenses/by/4.0/>).

1. Introduction

Basalt is mined and melted with no additives to fabricate filaments or fabrics. But not all basalts can be filamented, as its mineral and chemical levels differ by geographical area. A research report published by the Fraunhofer Institute for Microstructure of Materials and Systems, Germany, says that basalt fibers are a real alternative to glass fibers and carbon fibers. Birkner et al. [1] fabricated a novel silicatic polymer matrix that contains mineral glass fibers and basalt. The composite fabricated through the twin polymerization method demonstrated that 25% stiffness and 260% storage modulus increases can be gained from this material. Research from Bauer et al. [2] evaluated the performance of basalt fibers supplied by seven different companies in terms of crystallites, fiber chemistry, diameter distribution, and the occurrence of defects. The notable point from the authors is that mechanical strength is reduced by crystallites that act as defects in the fibers. Wolter et al. [3] investigated carbon-, glass-, and basalt-hybridized polybenzoxazine composites and reported that the inclusion of basalt increases the flame resistance characteristics. The interest in using composite materials in the construction industry and in marine, defense, and aerospace applications has increased considerably over the past few decades due to the materials' strength, tailorability, and strength-to-weight ratio. The crucial parameters such

as the thickness of laminates, fiber type, sequence of fiber laminates, boundary conditions, and resin matrix determine the impact response of fiber composites under varying loads. To this end, fiber hybridization provides tailored characteristics such as mechanical, electrical, and thermal properties with respect to primary and secondary reinforcements.

A study on flax- and basalt-fiber-reinforced vinyl ester resin matrix hybrid composites conducted by Fragassa et al. [4] reported that improved mechanical properties were obtained when basalt fibers were located in the outermost layers of the laminated composites. Masoud et al. [5] evaluated the impact of thickness in a basalt–Kevlar composite and reported the impact resistance of the composites. A study from Malik et al. [6] reveals that basalt rocks are the best to use in blast-resistant structural design as they have high compressive and fatigue resistance. Boria et al. [7] investigated flax- and basalt-reinforced thermoset vinyl ester composite for its impact resistance characteristics, and the authors observed 60% increase in impact resistance. A similar study conducted by Sarasini et al. [8,9] reported the post quasi-static impact test results of basalt–carbon-fiber-reinforced composites.

Zivkovic et al. [10] evaluated the impact energy and moisture absorption of basalt- and hybrid-flax-reinforced composites. Soares et al. [11] reported the advantages of reinforcing unsaturated polyester matrix with basalt fibers, where the variation in the distribution of the fiber–resin matrix showed reduced mechanical properties. Yuan et al. [12] evaluated the interfacial bonding and shear stress effects on basalt-fiber- and steel-fiber-reinforced concrete and reported that the use of steel fibers along with basalt fibers is better for concrete applications. Ferrante et al. [13] investigated and reported the low-velocity impact resistance of a basalt–glass fiber–aluminum composite. A study by Lapena et al. [14] reported that basalt fiber–glass fiber hybridization increased tensile strength by 45% and interlaminar shear strength by 11%. A study by Atmakuri et al. [15] on hybridization with basalt, E-glass, and graphite reported that hybrid fillers are better than single fibers. Also, they reported that basalt fibers have higher strength than glass fibers. Plappert et al. [16] reported the effect of surface modification using epoxysilane for the improvement of the fiber–matrix interface. Nayan [17], Vijayan et al. [18], and Natarajan et al. [19] revealed that the mechanical properties of laminated composites can be improved by managing the stacking sequence and arrangement of the fibers. Omid Sam-Daliri [20] developed glass fiber particle (1.75 mm filament)-reinforced polypropylene and assessed the mechanical properties through filament testing, and reported that the process methods and parameters significantly impact the properties of short-fiber-reinforced composites. In a similar vein, Yundong Ji [21] examined the flexural behavior of siloxane-modified epoxy/phenolic composites reinforced with glass fiber after heating. They reported that the addition of phenylpropylsiloxane-modified epoxy increased the room-temperature flexural strength by 70% and the post-heat flexural strength by 115%. In contrast, phenolic composites with dimethylsiloxane-modified epoxy exhibited a 44% reduction in room-temperature flexural strength, but a 117% increase in post-heat flexural strength.

In contrast, Yunfu [22] employed a unidirectional approach to examine the Weibull parameters of the material under different initial strain rates (25, 50, 100, and 200 s^{−1}) and six temperatures (Ω25, 0, 25, 50, 75, and 100 °C). The study found that the tensile strength increased linearly by approximately 49.1% within the strain rate range of 1/600–200 s^{−1}, while the toughness increased significantly (about 109.7%) when transitioning from quasi-static loading (1/600 s^{−1}) to dynamic loading (25 s^{−1}). There has been a surge in the use of polymer composites in a variety of technical sectors. On the other hand, the long-term service performance of such materials under harsh circumstances is still not well known, which hinders the development of designs that are both safe and economically efficient [23]. To enhance the physical and mechanical attributes of the material, Mario [24] conducted immersion experiments by combining carbon and basalt fiber. Throughout the experiment, it was discovered that FRP-LVL exhibits enhanced mechanical properties after being immersed in water for 48 h, particularly when bonded with PVAc adhesive. The PVAc-CF sample exhibited superior performance, with a 19% reduction in thickness swelling.

To this end, the authors of this research article aimed to investigate the stacking sequence of basalt–E-glass-reinforced polymer composite and report the characteristic effects of hybrid fiber reinforcement. Although research on various hybrid polymer composites has gained significant interest in the past decade, studies on basalt/E-glass-reinforced epoxy matrices still remain limited. Mechanical behavior such as flexural, tensile, and low-velocity impact properties and the thermal stability of the composite are presented and discussed.

2. Materials and Methods

2.1. Sample Preparation

Plain-woven E-glass and basalt-220.1270.P fabrics with areal densities of 240 g/m² and 160 g/m², respectively, were purchased from CF Composites, Mumbai, India, while the epoxy polymer matrix bi-component LY 556 and hardener W152 LR were purchased from a local supplier. The properties of the epoxy resin, basalt, and E-glass fabrics, as received from the supplier, are summarized in Tables 1 and 2.

Table 1. Properties of epoxy resin and hardener.

	Epoxy LY 556	Hardener W152 LR
Color	Pale yellow	Clear White
Specific gravity at RT	1.10–1.20	1.90–2.10
Viscosity [cps]	8000–12,000	16,000–18,000
Volatile content [wt. %]	0.75	1.0

Table 2. Properties of basalt and E-glass fabrics.

	Basalt	E-Glass
Density [g/cm ³]	2.40	1.95
Tensile strength [MPa]	3600–4850	3050–3600
Elastic modulus [GPa]	75–105	72–77
Elongation at break [%]	2.8	4.7
Maximum service temperature [°C]	345	380

Plain bidirectional woven basalt and glass fabrics were used in the proposed research in order to limit the laminate's slipperiness and delamination [25]. The epoxy resin and hardener were mixed and homogenized in a standard ratio of 3:1 in the pre-processing stage. The hybrid polymer composites with varying volume fractions of basalt and E-glass fibers (300 mm × 300 mm mold size) were fabricated using the vacuum-assisted resin transfer molding process (VARTM). Prior to the fabrication, wax was applied onto the base of the mold plate as a release agent. The basalt fiber fabric and E-glass fiber fabrics (300 mm × 300 mm) were arranged manually in the open mold one over the other up to the desired thickness of 3 mm. Once the fabrics were stacked, peel ply and breather fabric were placed over the stack and the entire setup was sealed using a polythene bag and sealant tape. The epoxy resin mixture was then allowed to flow through the fabric layers at a pressure of 0.1 bar. A vacuum pump at the pressure of 0.1 bar transferred the resin matrix from the reservoir and allowed the resin to flow through the fabric layers; excess resin was collected in a catching pot. Once the resin had evenly spread, the fabricated laminate was cured at room temperature for 24 h followed by heat treatment in a hot oven at 50 °C for 2 h.

For ease of understanding, the basalt fiber fabric and E-glass fiber fabric were designated as B and G, respectively. The fiber fabrics were stacked in the sequence of B-G-B-G-B-G-B-G-B, symmetric about neutral axis, where the basalt fiber fabric made up the outer

layer with the E-glass fiber fabric in the core. The fiber–matrix volume fractions of different hybrid configurations were calculated using Equation (1).

$$V_f = \frac{WB\&G/\rho_{\&G}}{\frac{W_m}{\rho_m} + \frac{W_B+W_G}{\rho_B+\rho_G}} \quad (1)$$

where: f —fiber, m —matrix, W —weight, ρ —density, B —basalt fiber, G —E-glass fiber.

Table 3 summarizes the thickness of the laminates and the various volume fractions of the basalt/E-glass/epoxy polymer configurations. Designation PC303040 refers to the polymer composite (PC) with 30 vol. % of epoxy matrix, 30 vol. % basalt, and 40 vol. % of E-glass. The specimens were then cut using water jet machining for various mechanical tests as per ASTM standards. Figure 1 shows a schematic representation of the stacking and fabricated samples.

Table 3. Thickness and volume fraction of hybrid configurations.

Designation	Thickness [mm]	Epoxy Matrix [vol. %]	Basalt [vol. %]	E-Glass [vol. %]
PC303040	3.2	30	30	40
PC303337	3.1	30	33	37
PC303733	3.2	30	37	33
PC313534	3.4	31	35	34
PC323929	3.3	32	39	29

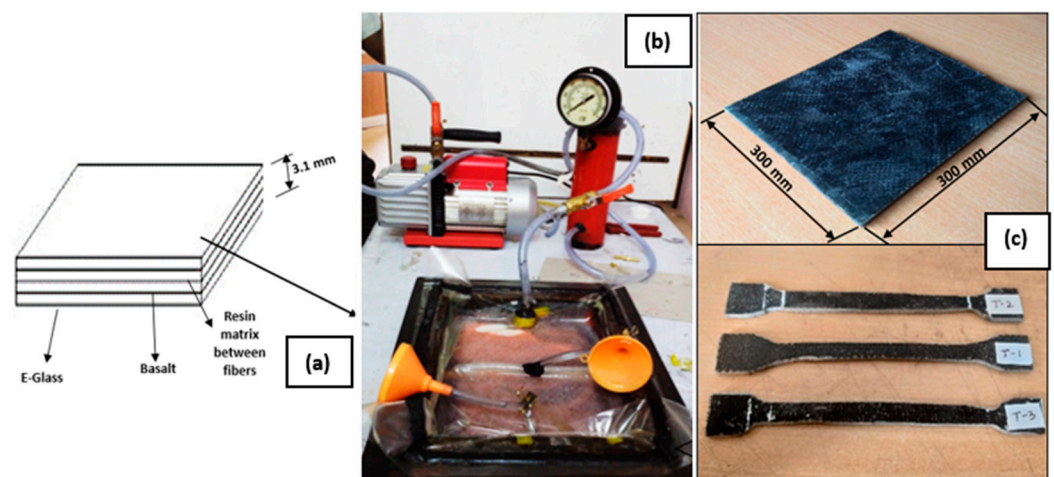


Figure 1. (a) Schematic representation of stacking sequence. (b) Vacuum bag setup. (c) Basalt/E-glass polymer composite samples.

2.2. Method of Research

Uniaxial tensile test specimens were prepared as per the ASTM D638 standard [26] and tests were performed using a servo-controlled universal testing machine (Instron 8801) Norwood, MA, US with a speed rate of 0.001 to 1.000 mm/min, ± 100 kN (22,500 lbf) axial force capacity, and patented dynacell load cell feature compensation for inertial loads caused by heavy grips and fixtures. Three samples were tested in each configuration to measure the tensile strength, yield strength, and ductility. Flexural specimens, as per ASTM D790 (80 mm \times 13 mm \times 3 mm) standards [27], were tested using the same machine at a cross head speed of 4 mm/min. In order to analyze the effect of impact load on the specimens in both horizontal and vertical conditions, both Izod and Charpy tests were conducted. An Izod test, as per ASTM D256 [28], and a Charpy test, as per ASTM D6110 [29], were conducted using an AIT-300N impact tester with 600 mm of pendulum swing, 18.7 kg striking hammer weight, and up to 10 m/s of impact velocity. Field-Emission Scanning Electron Microscopy (FE-SEM) was used to analyze the fractured samples to

understand the failure due to load at different magnifications. Thermogravimetric analysis was performed (model: PerkinElmer 2.0, TGA 4000, optimized with Pyris Software) at a maximum temperature of 600 °C in order to calculate the mass changes with respect to the raise in temperature.

3. Results

3.1. Tensile Test

Figure 2 shows the ultimate tensile stress and percentage strain values of all five configurations upon tensile loading at a 0.1 s⁻¹ strain rate. PC323929 (E-glass fiber: 29 vol. %) has the lowest tensile strength of 103.61 MPa, while PC303040 (E-glass fiber: 40 vol. %) has the highest tensile strength of 185.19 MPa. The results show that the strain to corresponding tensile stress varies gradually over an increase in the volume of E-glass fiber. The 78.73% improvement in tensile strength can be attributed to the reinforcing effect of the E-glass fiber; when polymer composites are subjected to loading, the glass fibers act as load carriers to transfer the load from the matrix along the fibers [25]. Long-Cheng Tang et al. [30] reported that neat epoxy possesses about 66 MPa tensile strength, which is around 300 % lower than PC303040. This, in turn, results in uniform stress distribution and, hence, the enhanced strength of the composite. It is also noteworthy that a higher reinforcement of basalt into the matrix restricts the tensile ability of the composite. A loss of ductility was also observed in PC323929 (basalt 39 vol. %) where it was nearly 83% lower in strength than PC303040, which could be due to the lower Si content in the basalt. The current research findings are different from some published results [31] where either basalt fibers or E-glass fibers were used. Though these authors reported that the tensile strength of basalt-fiber-reinforced epoxy composite is higher than that of E-glass-fiber-reinforced composite, the combination of basalt and E-glass fabrics with different proportions along with the epoxy matrix greatly impacts the stiffness of the basalt fabrics. The hybrid composite results in a higher resistance to pulling forces before the material succumbs to that force [30].

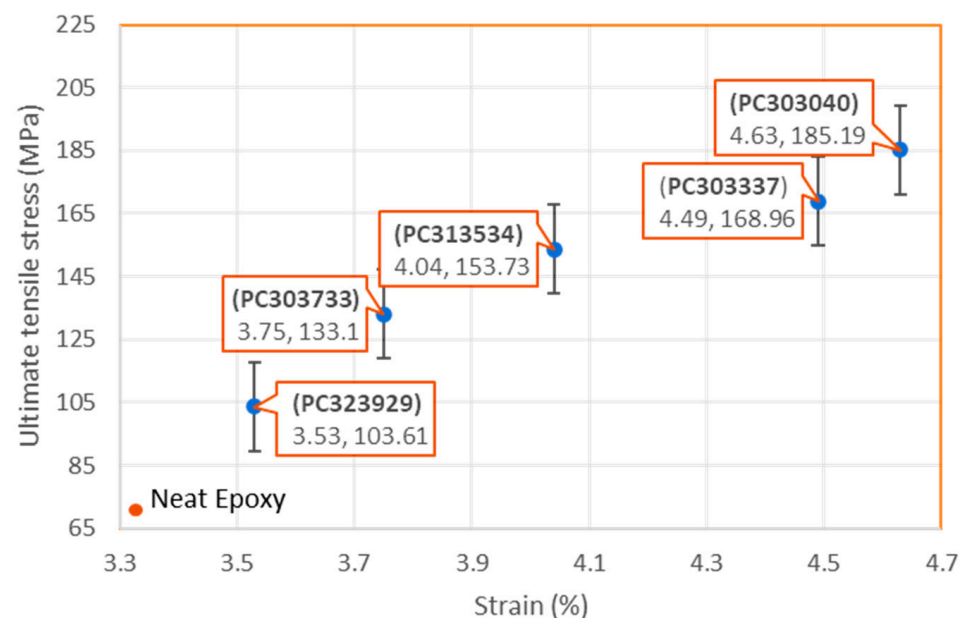


Figure 2. Stress strain after tensile testing of the hybrid samples.

3.2. Flexural Test

Figure 3 shows the flexural strength of the composites with varying filler compositions. From Figure 3, it can be seen that PC303040 (E-glass 40 vol. %) showed the highest bending strength of 227.87 MPa and the highest bending strain of 3.39%. The reported flexural strength of the composite is \approx 128% higher than neat epoxy, which has a flexural strength

of 99.88 MPa. In fact, it can be observed that all composites exhibited higher flexural strength than neat epoxy. The reported flexural strength was attained at the maximum filler content of E-glass fiber (i.e., 40 vol. %), but at the lowest concentration of basalt fiber, i.e., 30 vol. %. An increase in the basalt fiber content in the polymer reduced the flexural properties of the composite. This could be due to excess fiber content, which restricts excellent interfacial adhesion and tends to be non-homogeneously distributed, which, in turn, leads to agglomeration. The agglomeration of the fiber results in defects in the internal structure and counteracts the function of the fiber to reinforce the polymer matrix, thus decreasing the strength. Xiane Xiao [32] reported the flexural strength of neat epoxy (81 MPa), which is included in Figure 3 for comparison.

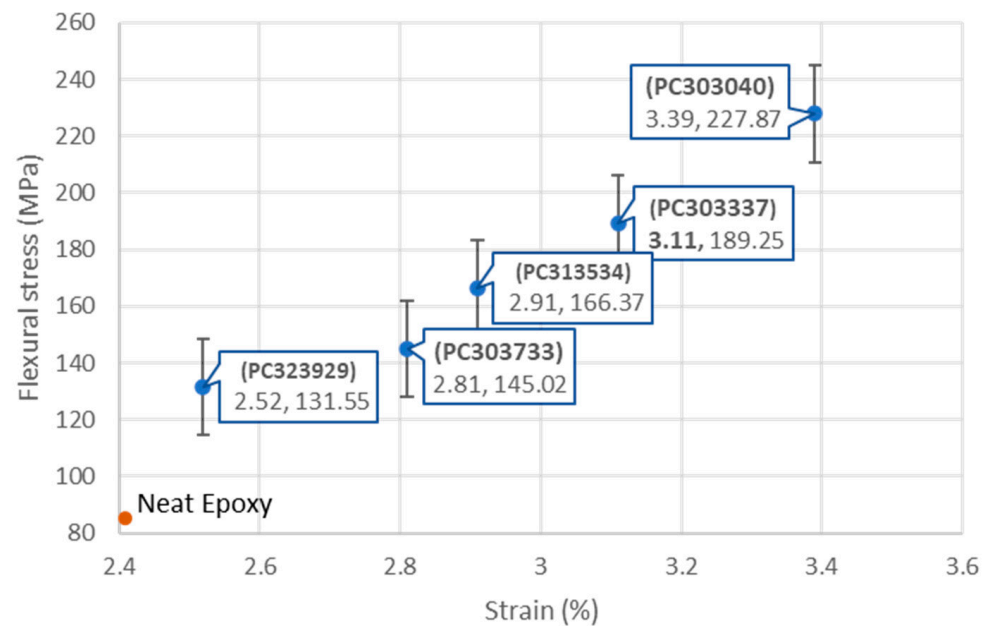


Figure 3. Stress–strain after bending load of the hybrid samples.

3.3. Low-Velocity Impact Test

Figure 4 shows the test procedure and broken samples after Izod and Charpy impact testing, while the corresponding results are summarized in Table 4. The energy absorption of the laminates gradually increased with the increase in the basalt fiber reinforcement. Similarly, the Charpy impact testing revealed that the hybrid laminate with 39 vol. % basalt showed better energy absorption than the other laminates. During Izod impact testing, the energy of the pendulum is transferred to the polymer composite being tested, and part of this energy is consumed during fracture. The fracture cumulatively undergoes the energy dissipation mechanism due to fiber–matrix interactions such as sliding, debonding, or fiber pull-out. In the present study, the Izod test results show that the higher reinforcement of basalt fiber exhibits better impact energy absorption capability. The 10 vol. % basalt fiber used as reinforcement in the polymer composite improved the Charpy and Izod impact energy absorption by 40–50% and 60–70%, respectively.

It can be postulated that uneven surfaces with striations in basalt fiber may enhance interfacial bonding between the fiber and the polymer matrix. Moreover, SEM images of fractured surfaces (discussed in Section Fracture Surface Analysis) indicate significant debonding and pull-out of fibers, both of which represent an energy dissipation mechanism that can lead to the enhanced impact strength at higher basalt fiber contents. On the other hand, it was noticed that there is lack of impact energy absorption in composite reinforced with 35 vol. % basalt fiber, which may be due to the void or fiber peel-off that may have occurred during the testing or pre-processing stages.

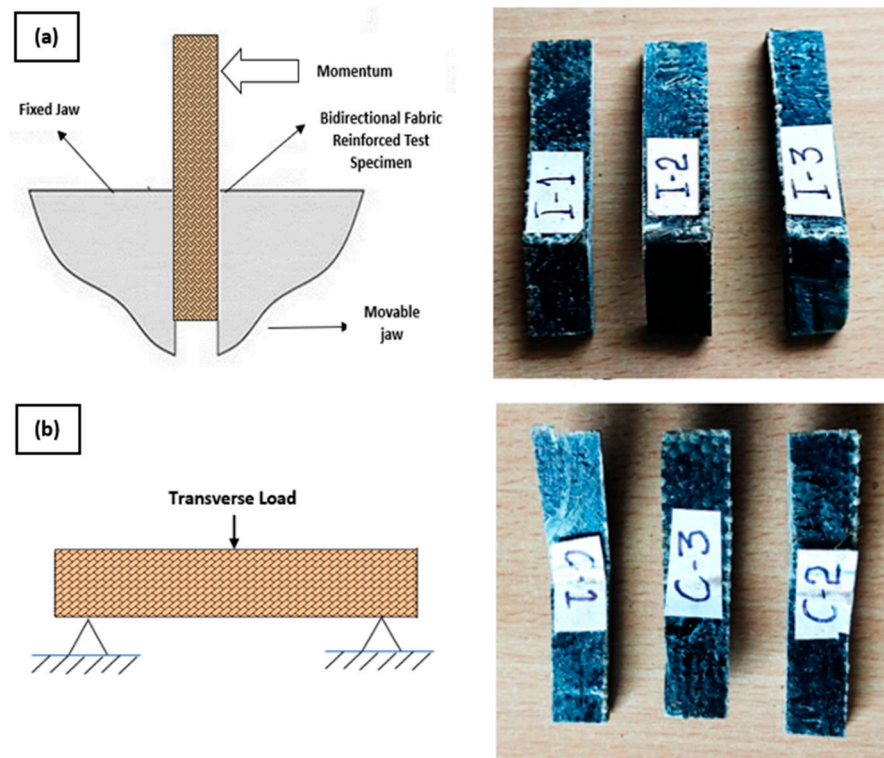


Figure 4. (a) Illustration of Izod impact test and broken samples. (b) Illustration of Charpy test and broken sample.

Table 4. Energy absorption of along fiber orientations.

Sample Code	Energy Absorption along Horizontal Fiber Orientation [J]	Energy Absorption along Vertical Fiber Orientation [J]
PC303040	3.1	4.6
PC303337	3.3	4.8
PC303733	3	5.5
PC313534	3.9	6.1
PC323929	4.5	7.8

3.4. Thermogravimetric Analysis

Figure 5 shows the Thermal Gravimetric Analysis (TGA) of hybrid basalt/E-glass-fiber-reinforced polymer composites. From Figure 5, it can be seen that all composites reinforced with basalt/E-glass fibers displayed good thermal stability. For example, less than 5% weight loss was reported when all composites were gradually heated up to 320 °C, while less than 10% weight loss was reported for all samples when heated up to 400 °C. However, it is noteworthy that varying the composition of basalt or E-glass fiber had a significant effect on the glass transition temperature (T_g) of the composites, which indicates a possible effect on the physical properties of the composite as well.

For instance, the T_g of PC303040 (E-glass fiber: 40 vol. %) was 369.1 °C, while the T_g of PC 323929 (E-glass fiber: 29 vol. %) was 328.3 °C (i.e., approximately 12.43% higher). The increase in T_g for PC303040 can be attributed to the greater amount of E-glass fiber used; the E-glass fibers effectively restricted the segmental motion of the polymer matrix due to excellent interfacial adhesion with the epoxy matrix. A lower amount of E-glass fiber reinforcement (i.e., 29 vol. %, 33 vol. %, and 34 vol. % E-glass fibers) did not show a significant difference in T_g since the E-glass fiber amount was insufficient to slow down or hinder the molecular dynamics of the composite, which can alter the T_g of hybrid basalt/E-glass-fiber-reinforced polymer composites.

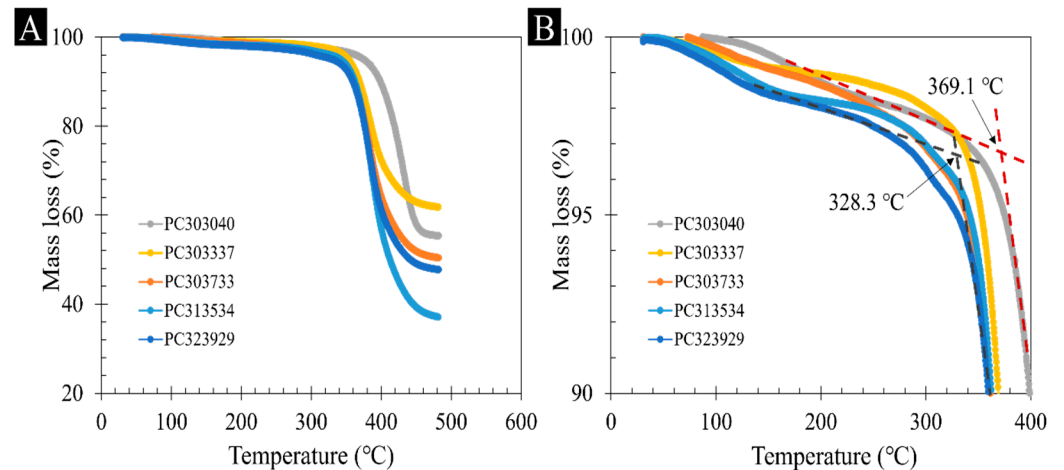


Figure 5. (A) Thermal Gravimetric Analysis (TGA) of hybrid basalt/E-glass fiber composites with varying E-glass fiber content. (B) Magnified version of TGA curve to show significant weight loss from 300 °C to 400 °C.

4. Discussion

Figure 6 shows the Ashby scatter plot used to accurately describe and categorize the materials based on their strength-to-weight ratio. Most of the hybrid-fiber-reinforced polymer composites investigated in the present study lie within the composite material region. For instance, composite PC303040 showed a strength-to-weight ratio comparable to glass-fiber-reinforced composites (GFRPs). As a result of the higher strength-to-weight ratio, E-glass–epoxy composites typically show a reasonable degree of flexibility and superior tensile strength. In addition, due to the enhanced modulus of elasticity, basalt fiber also shows greater resistance to fracturing, deformation, and ballistic loading. However, it is noteworthy that the results from the present study can be further improved to achieve composites that consistently show a higher strength-to-weight ratio (i.e., higher than GFRPs) and, in turn, reveal a previously unknown material feature.

The findings from the tensile and flexural studies indicate that increasing the proportion of E-glass fiber improved the tensile and flexural strength, while increasing the fraction of basalt improved resilience to impact. This is because the proposed laminates show both malleable and durable properties. In another study by Elmahdy et al. [33], the properties of woven basalt and E-glass-fiber-reinforced epoxy composites were compared at high strain rates in order to supplement them for auxiliary structural elements of aircraft. The hybridization of basalt and E-glass fiber may enhance the properties of the composite, which can be advantageous for tertiary parts used in aerospace applications.

Fracture Surface Analysis

The fracture analysis using FE-SEM in the present study was conducted on the composite containing 40 vol. % E-glass fiber (PC303040), since this composite exhibits the optimum tensile and flexural properties. Figure 7 shows that the fiber fracture orientations and various defects of basalt fiber and E-glass fiber composites were indicated clearly at magnifications of $250\times$ – $1000\times$. From the SEM images, several defects and failure mechanisms were noticed in the composite, such as voids, pores, fiber pull-outs, and rough matrix surfaces. The findings from the SEM analysis indicate that an increase in the volume percentage of basalt leads to the deterioration of interfacial bonding between the polymer matrix and the reinforcement, as well as an increase in breakdown and the expansion of cracks [34]. Moreover, the increased flexibility suggests the presence of a well-established matrix support connection and favorable wettability. The observed trend can be attributed to the prior treatment and curing process of E-glass and basalt fibers before incorporating them in the polymer matrix [26].

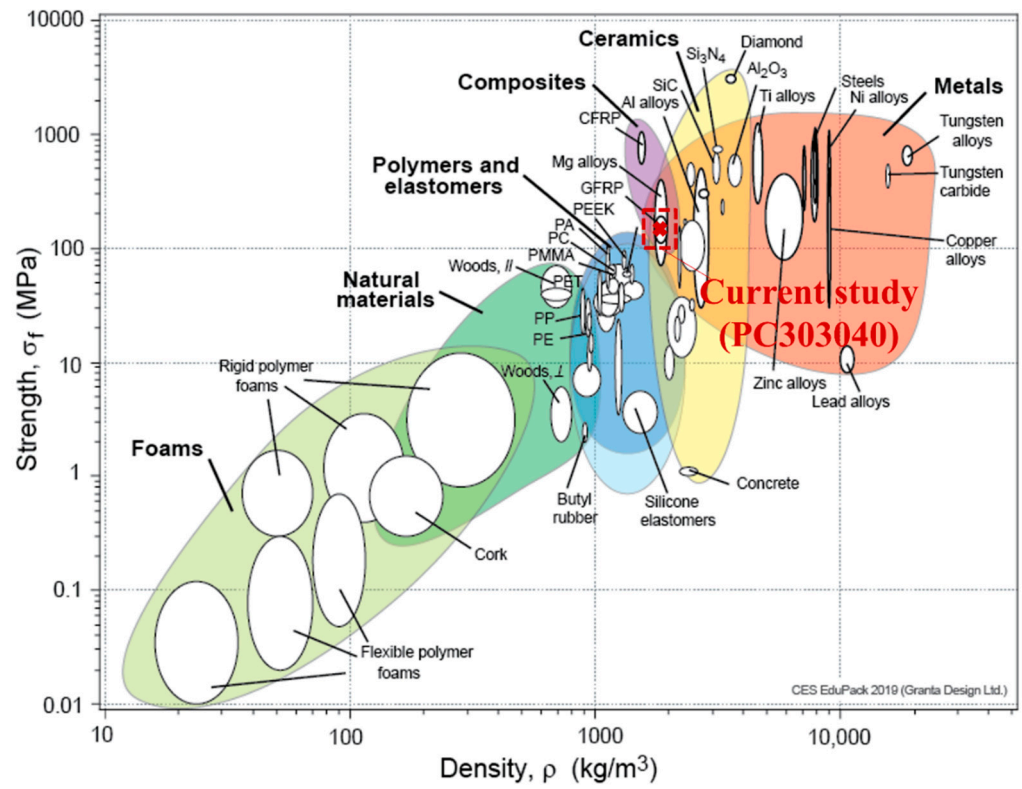


Figure 6. Experimental data representation—Ashby chart.

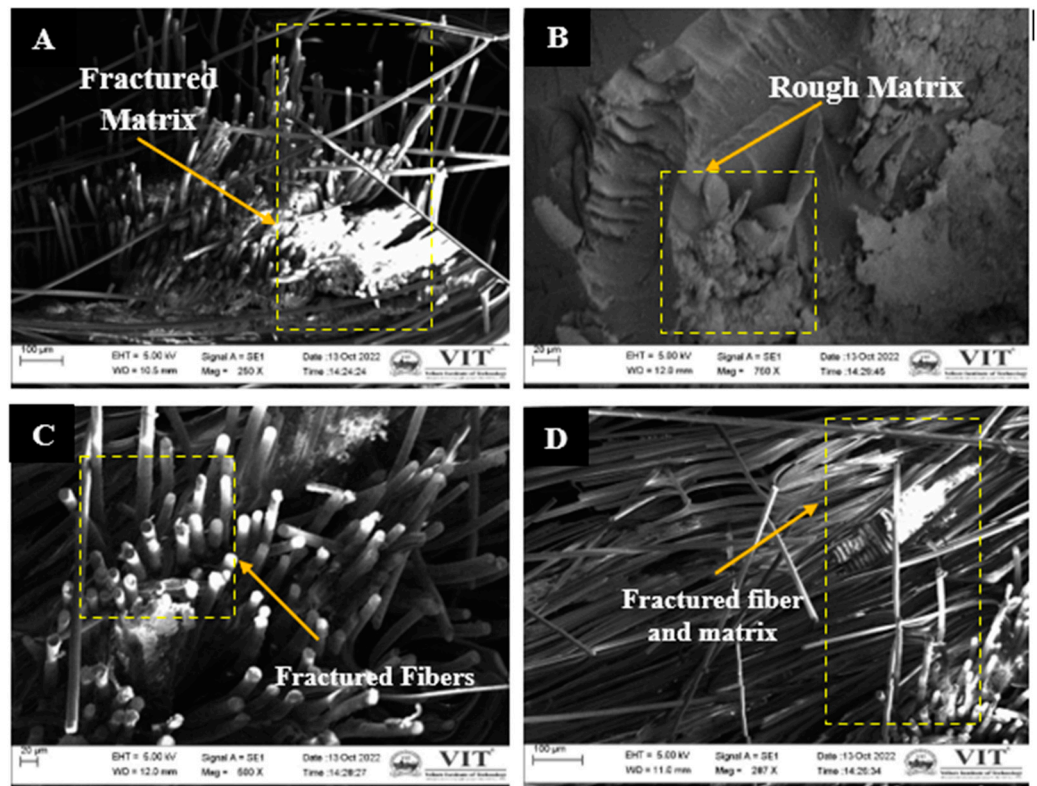


Figure 7. FE-SEM images of 40% E-glass reinforced composites (PC303040), (A) Fractured matrix surface, (B) Rough matrix surface, (C) Fractured fibers, (D) Fractured matrix and fibers.

5. Conclusions

Hybrid basalt/E-glass-fiber-reinforced polymer composites with varying fiber fractions were fabricated using vacuum-assisted resin transfer molding (VARTM).

- The experimental results showed that a 10% higher volume fraction of basalt fiber provides excellent impact energy absorption, i.e., 40–70%.
- The tensile test results revealed that 40 vol. % E-glass fiber as reinforcement shows better tensile strength than 40 vol. % basalt-fiber-reinforced composites.
- Similarly, the three-point bending flexural test results depicted that a higher volume fraction of E-glass fiber provides reasonable flexural strength, i.e., 80% higher than other fabricated laminates.
- The analysis of the results allowed to conclude that 40 vol. % E-glass-fiber-reinforced composites are better for tensile and flexural conditions, while 40 vol. % basalt-reinforced composites are better for applications involving impact energy.
- During the thermogravimetric analysis, it was noticed that PC313534 (35 vol. % basalt and 34 vol. % E-glass) possesses the lowest decomposition temperature of 381.1 °C. Similarly, samples with basalt and E-glass fiber in almost equal quantities (PC313534—35 vol. % basalt and 34 vol. % E-glass) provide better thermal stability than other compositions.
- The outcome from the present study can be used in designing composite materials that exhibit high strength-to-weight ratio, which can be useful in defense armors and aerospace applications such as flaps, slats, and fuselages.

Author Contributions: Conceptualization, Methodology, E.N., G.F., C.K.A.; Software, S.M.S.; Validation, E.N.; Resources, G.F.; Data curation, E.N.; Writing—original draft, S.M.S.; Writing—review & editing, K.M., G.F., C.K.A.; Supervision, C.K.A.; Project administration, E.N. and G.F.; Funding acquisition, G.F. All authors have read and agreed to the published version of the manuscript.

Funding: This research received no external funding.

Data Availability Statement: The data presented in this study are available within the article.

Conflicts of Interest: The authors declare that they have no known competing financial interests or personal relationships that could have appeared to influence the work reported in this paper.

References

1. Birkner, M.; Spange, S.; Koschek, K. Basalt fiber reinforced polymers with improved thermal and mechanical properties by combination of twin polymerization with epoxide chemistry. *Polym. Compos.* **2019**, *40*, 3115–3121. [[CrossRef](#)]
2. Bauer, F.; Kempf, M.; Weiland, F.; Middendorf, P. Structure-property relationships of basalt fibers for high performance applications. *Compos. B Eng.* **2018**, *145*, 121–128. [[CrossRef](#)]
3. Wolter, N.; Beber, V.C.; Sandinge, A.; Blomqvist, P.; Goethals, F.; Van Hove, M. Carbon, Glass and Basalt Fiber Reinforced Polybenzoxazine: The Effects of Fiber Reinforcement on Mechanical, Fire, Smoke and Toxicity Properties. *Polymers* **2020**, *12*, 2379. [[CrossRef](#)]
4. Fragassa, C.; Pavlovic, A.; Santulli, C. Mechanical and impact characterisation of flax and basalt fibre vinylester composites and their hybrids. *Compos. B Eng.* **2018**, *137*, 247–259. [[CrossRef](#)]
5. Khazaie, M.; Eslami-Farsani, R.; Saeedi, A. Evaluation of repeated high velocity impact on polymer-based composites reinforced with basalt and Kevlar fibers. *Mater. Today. Commun.* **2018**, *17*, 76–81. [[CrossRef](#)]
6. Malik, A.; Chakraborty, T.; Rao, K.S. Strain rate effect on the mechanical behavior of basalt: Observations from static and dynamic tests. *Thin-Walled Struct.* **2018**, *126*, 127–137. [[CrossRef](#)]
7. Boria, S.; Pavlovic, A.; Fragassa, C.; Santulli, C. Modeling of Falling Weight Impact Behavior of Hybrid Basalt/Flax Vinylester Composites. *Procedia Eng.* **2016**, *167*, 223–230. [[CrossRef](#)]
8. Sarasini, F.; Tirillò, J.; Ferrante, L.; Valente, M.; Valente, T.; Lampani, L. Drop-weight impact behaviour of woven hybrid basalt-carbon/epoxy composites. *Compos. B Eng.* **2014**, *59*, 204–220. [[CrossRef](#)]
9. Sarasini, F.; Tirillò, J.; Valente, M.; Valente, T.; Cioffi, S.; Iannace, S. Effect of basalt fiber hybridization on the impact behavior under low impact velocity of glass/basalt woven fabric/epoxy resin composites. *Compos. A Appl. Sci. Manuf.* **2013**, *47*, 109–123. [[CrossRef](#)]

10. Živković, I.; Fragassa, C.; Pavlović, A.; Brugo, T. Influence of moisture absorption on the impact properties of flax, basalt and hybrid flax/basalt fiber reinforced green composites. *Compos. B Eng.* **2017**, *111*, 148–164. [[CrossRef](#)]
11. Soares, B.; Preto, R.; Sousa, L.; Reis, L. Mechanical behavior of basalt fibers in a basalt-UP composite. *Procedia Struct. Integr.* **2016**, *1*, 82–89. [[CrossRef](#)]
12. Yuan, C.; Chen, W.; Pham, T.M.; Hao, H. Bond behavior between basalt fibres reinforced polymer sheets and steel fibres reinforced concrete. *Eng. Struct.* **2018**, *176*, 812–824. [[CrossRef](#)]
13. Ferrante, L.; Sarasini, F.; Tirillò, J.; Lampani, L.; Valente, T.; Gaudenzi, P. Low velocity impact response of basalt-aluminium fibre metal laminates. *Mater. Des.* **2016**, *98*, 98–107. [[CrossRef](#)]
14. Lapena, M.H.; Marinucci, G. Mechanical Characterization of Basalt and Glass Fiber Epoxy Composite Tube. *Mater. Res.* **2017**, *21*, e20170324. [[CrossRef](#)]
15. Atmakuri, A.; Kolli, L.; Palevicius, A.; Urbaite, S.; Janusas, G. Influence of Filler Materials on Wettability and Mechanical Properties of Basalt/E-Glass Woven Fabric-Reinforced Composites for Microfluidics. *Micromachines* **2022**, *13*, 1875. [[CrossRef](#)]
16. Plappert, D.; Ganzenmüller, G.C.; May, M.; Beisel, S. Mechanical Properties of a Unidirectional Basalt-Fiber/Epoxy Composite. *J. Compos. Sci.* **2020**, *4*, 101. [[CrossRef](#)]
17. Patel, N. Investigations on Mechanical Strength of Hybrid Basalt/Glass Polyester Composites. *Int. J. Appl. Eng.* **2018**, *13*, 4083–4088.
18. Vijayan, R.; Natarajan, E.; Palanikumar, K.; Krishnamoorthy, A.; Markandan, K.; Ramesh, S. Effect of hybridization and stacking sequences on mechanical properties and thermal stability of aloe vera-roselle-glass fiber reinforced polymer composites. *Polym. Compos.* **2023**, *44*, 6593–6603. [[CrossRef](#)]
19. Natarajan, E.; Freitas, L.I.; Santhosh, M.S.; Markandan, K.; Majeed Al-Talib, A.A.; Hassan, C.S. Experimental and numerical analysis on suitability of S-Glass-Carbon fiber reinforced polymer composites for submarine hull. *Def. Technol.* **2023**, *19*, 1–11. [[CrossRef](#)]
20. Sam-Daliri, O.; Ghabezi, P.; Flanagan, T.; Finnegan, W.; Mitchell, S.; Harrison, N. Recovery of Particle Reinforced Composite 3D Printing Filament from Recycled Industrial Polypropylene and Glass Fibre Waste. In Proceedings of the 8th World Congress on Mechanical, Chemical, and Material Engineering (MCM'22), Prague, Czech Republic, 31 July–2 August 2022. [[CrossRef](#)]
21. Ji, Y.; Zhang, X.; Wang, C.; Li, S.; Cao, D. Post-Heat Flexural Properties of Siloxane-Modified Epoxy/Phenolic Composites Reinforced by Glass Fiber. *Polymers* **2024**, *16*, 708. [[CrossRef](#)]
22. Ou, Y.; Zhu, D.; Zhang, H.; Huang, L.; Yao, Y.; Li, G.; Mobasher, B. Mechanical Characterization of the Tensile Properties of Glass Fiber and Its Reinforced Polymer (GFRP) Composite under Varying Strain Rates and Temperatures. *Polymers* **2016**, *8*, 196. [[CrossRef](#)] [[PubMed](#)]
23. Uthaman, A.; Xian, G.; Thomas, S.; Wang, Y.; Zheng, Q.; Liu, X. Durability of an Epoxy Resin and Its Carbon Fiber- Reinforced Polymer Composite upon Immersion in Water, Acidic, and Alkaline Solutions. *Polymers* **2020**, *12*, 614. [[CrossRef](#)]
24. Núñez-Decap, M.; Sandoval-Valderrama, B.; Opazo-Carlsson, C.; Moya-Rojas, B.; Vidal-Vega, M.; Opazo-Vega, A. Use of Carbon and Basalt Fibers with Adhesives to Improve Physical and Mechanical Properties of Laminated Veneer Lumber. *Appl. Sci.* **2023**, *13*, 10032. [[CrossRef](#)]
25. Santhosh, M.S.; Sasikumar, R.; Khadar, S.D.A.; Natrayan, L. Ammonium Polyphosphate Reinforced E-Glass/Phenolic Hybrid Composites for Primary E-Vehicle Battery Casings –A Study on Fire Performance. *J. New Mater. Electrochem. Syst.* **2021**, *24*, 247–253. [[CrossRef](#)]
26. Santhosh, M.S.; Sasikumar, R.; Natarajan, E. E-Glass/phenolic matrix/APP laminate as a potential candidate for battery casing of e-vehicle—Experimental investigations. *Mater. Res. Express.* **2021**, *8*, 045310. [[CrossRef](#)]
27. *ASTM D790*; Standard Test Methods for Flexural Properties of Unreinforced and Reinforced Plastics and Electrical Insulating Materials. ASTM International: West Conshohocken, PA, USA, 2017.
28. *ASTM D256*; Standard Test Methods for Determining the Izod Pendulum Impact Resistance of Plastics. ASTM International: West Conshohocken, PA, USA, 2023.
29. *ASTM D6110*; Standard Test Method for Determining the Charpy Impact Resistance of Notched Specimens of Plastics. ASTM International: West Conshohocken, PA, USA, 2018.
30. Gong, L.-X.; Zhao, L.; Tang, L.-C.; Liu, H.-Y.; Mai, Y.-W. Balanced electrical, thermal and mechanical properties of epoxy composites filled with chemically reduced graphene oxide and rubber nanoparticles. *Compos. Sci. Technol.* **2015**, *121*, 104–114. [[CrossRef](#)]
31. Liu, J.; Chen, M.; Yang, J.; Wu, Z. Study on Mechanical Properties of Basalt Fibers Superior to E-glass Fibers. *J. Nat. Fibers* **2022**, *19*, 882–894. [[CrossRef](#)]
32. Xiao, X.; Lu, S.; Qi, B.; Zeng, C.; Yuan, Z.; Yu, Y. Enhancing the thermal and mechanical properties of epoxy resins by addition of a hyperbranched aromatic polyamide grown on microcrystalline cellulose fibers. *RSC Adv.* **2014**, *4*, 14928. [[CrossRef](#)]

33. Elmahdy, A.; Verleysen, P. Mechanical behavior of basalt and glass textile composites at high strain rates: A comparison. *Polym. Test.* **2020**, *81*, 106224. [[CrossRef](#)]
34. McNiffe, E.; Ritter, T.; Higgins, T.; Sam-Daliri, O.; Flanagan, T.; Walls, M.; Ghabezi, P.; Finnegan, W.; Mitchell, S.; Harrison, N.M. Advancements in Functionally Graded Polyether Ether Ketone Components: Design, Manufacturing, and Characterisation Using a Modified 3D Printer. *Polymers* **2023**, *15*, 2992. [[CrossRef](#)]

Disclaimer/Publisher's Note: The statements, opinions and data contained in all publications are solely those of the individual author(s) and contributor(s) and not of MDPI and/or the editor(s). MDPI and/or the editor(s) disclaim responsibility for any injury to people or property resulting from any ideas, methods, instructions or products referred to in the content.